

# Molecular photoionization cross sections in electron propagator theory: Angular distributions beyond the dipole approximation

G. M. Seabra

Department of Chemistry, Kansas State University, Manhattan, Kansas, 66506-3701

I. G. Kaplan

Instituto de Investigaciones en Materiales, Universidad Nacional Autónoma de México, Apartado Postal 70-360, México, Distrito Federal 04510, México

J. V. Ortiz<sup>a)</sup>

Department of Chemistry, Kansas State University, Manhattan, Kansas, 66506-3701

(Received 28 July 2005; accepted 3 August 2005; published online 22 September 2005)

Corrections to dipole approximation results for angular distributions in photoionization of first-row hydrides have determined by using Dyson orbitals calculated with *ab initio* electron propagator theory and by considering the full multipole expansion for the incident photon representation. The relative importance of first-order corrections which consist of electric quadrupole and magnetic dipole terms and of higher-order terms has been estimated as a function of photon energy. Multipole corrections to the dipole approximation depend on photon energy and on the characteristics of the Dyson orbitals. © 2005 American Institute of Physics. [DOI: 10.1063/1.2043087]

## I. INTRODUCTION

Angle-resolved photoelectron spectroscopy has become an important and powerful instrument for the study of the electronic structure of atoms, molecules, and solids. To interpret these experiments, photoionization cross sections are calculated in the first order of time-dependent perturbation theory. The perturbation operator (for the interaction of photons with the electrons of the target) is usually represented in the so-called dipole approximation (DA),<sup>1-4</sup> which is valid for radiation with wavelength  $\lambda$  that is considerably larger than the target size. In this case, the electromagnetic field practically does not change over the spatial extent of the target's charge distribution.

The interaction energy of a flow of photons, possessing the wave vector  $\mathbf{k}_{\text{ph}}$  and the polarization vector  $\mathbf{n}$ , with some arbitrary,  $N$ -electron system is described by the operator<sup>1,2</sup>

$$V_{\text{int}} = -\frac{e}{m_e c} A_0 \mathbf{n} \sum_{i=1}^N e^{i\mathbf{k}_{\text{ph}} \cdot \mathbf{r}_i} \mathbf{p}_i \quad (1)$$

where  $c$  is the speed of light,  $e$  and  $m_e$  are, respectively, the charge and mass of an electron,  $\mathbf{r}_i$  and  $\mathbf{p}_i = -i\hbar \nabla_i$  are, respectively, the position vector and the momentum operator of  $i$ th electron, and  $A_0$  is the amplitude of the vector potential of the electromagnetic field.

In the DA, the expansion

$$e^{i\mathbf{k} \cdot \mathbf{r}} = 1 + i\mathbf{k} \cdot \mathbf{r} - \frac{1}{2}(\mathbf{k} \cdot \mathbf{r})^2 + \dots \quad (2)$$

is truncated after the first term. This approximation is valid if  $kr \ll 1$ , where  $r$  is of the order of the linear size of the target.

Taking into account that  $k=2\pi/\lambda$ , the condition for the DA can be written as

$$kr = \frac{2\pi}{\lambda} r \ll 1,$$

or

$$\lambda \gg 2\pi r. \quad (3)$$

For small molecules,  $r \approx 1 \text{ \AA}$  and, according to Eq. (3),  $\lambda$  must be much larger than  $2\pi$ . Thus, the condition of Eq. (3) is fulfilled for  $\lambda > 60 \text{ \AA}$ , or  $E_{\text{ph}} < 200 \text{ eV}$  [ $E(\text{eV}) = 12384/\lambda(\text{\AA})$ ]. For large polyatomic molecules, the multipole effects can manifest themselves at photon energies even smaller than 200 eV. Note that the breakdown of the DA has usually been estimated to occur for  $E_{\text{ph}} > 1 \text{ keV}$ .<sup>5</sup>

In the DA, the angular distribution of photoelectrons for linearly polarized light is presented as<sup>6</sup>

$$\frac{d\sigma(\theta)}{d\Omega_e} = \frac{\sigma}{4\pi} [1 + \beta P_2(\cos \theta)], \quad (4)$$

where  $\sigma$  is the total cross section,  $\Omega_e$  is the solid angle in the direction of the ejected electron,  $\theta$  is the angle between the direction of the ejected electron and the photon polarization vector,  $\beta$  is an asymmetry parameter depending upon the angular momentum of an atomic shell, and  $P_2(x) = \frac{1}{2}(3x^2 - 1)$  is the second-order Legendre polynomial.

At large photon energies, the DA is no longer valid. As was shown in Refs. 7 and 8 in the general case, the angular distribution of photoelectrons from a particular atomic subshell for unpolarized light can be expressed as a linear combination of the Legendre polynomials,

<sup>a)</sup>Electronic mail ortiz@ksu.edu

$$\frac{d\sigma(\Theta)}{d\Omega_e} = \frac{\sigma}{4\pi} \sum_n B_n P_n(\cos \Theta), \quad (5)$$

where  $\Theta$  is the angle between the photon and electron propagation vectors. If the expansion of Eq. (2) is truncated after the electric quadrupole ( $E2$ ) and magnetic dipole ( $M1$ ) terms, the angular distribution of Eq. (5) can be presented in terms of three parameters<sup>9-12</sup>

$$\frac{d\sigma(\Theta)}{d\Omega_e} = \frac{\sigma}{4\pi} \left[ 1 - \frac{\beta}{4} (3 \cos^2 \Theta - 1) + \left( \frac{\gamma}{2} \sin^2 \Theta + \delta \right) \cos \Theta \right], \quad (6)$$

where  $\beta$ ,  $\gamma$ , and  $\delta$  are the electric dipole, electric quadrupole, and magnetic dipole asymmetry parameters, respectively. If the nondipole terms are neglected, Eq. (6) yields the equivalent of Eq. (4) for unpolarized light.<sup>13</sup>

It follows from Eq. (6) that the nondipole terms essentially change the angular distribution. At  $\Theta = 54.74^\circ$ , the dipole angular distribution of the photoelectrons is completely determined by the nondipole terms.

The first measurements of multipole effects in atomic photoionization were reported in Refs. 14 and 15, where the deviations from the DA were detected at energies below 5 keV. An analysis of experimental and theoretical studies of atomic photoionization is presented in the review by Lindle and Hemmers.<sup>16</sup> (See also Refs. 17 and 18.)

The first experiments reporting the measurements of multipole angular distribution in molecules were published in 2001.<sup>19</sup> Irradiation at  $E_{\text{ph}} \leq 500$  eV of gas-phase  $\text{N}_2$  molecules revealed large multipole effects in the angular distribution of  $K$ -shell photoelectrons. The authors remarked that these effects were observed at energies as low as 500 eV. However, according to our estimate in Eq. (3), multipole effects in the photoionization of small molecules can be expected for  $E_{\text{ph}} > 200$  eV.

Experiments on fixed-in-space  $\text{N}_2$  molecules<sup>20</sup> demonstrated a pronounced azimuthal structure in the angular distribution of ejected electrons. Langhoff *et al.*<sup>21,22</sup> derived a theory for fixed-in-space molecules that includes, as in Eq. (6),  $E1$ ,  $E2$  and  $M2$  multipoles. Comparison of the measured spectra with this theory led the authors of this work<sup>20</sup> to conclude that terms of higher order are needed to describe the observed structure in the azimuthal dependence.

Recently, Grum-Grzhimailo<sup>23</sup> formulated a general theory of angular distribution of molecular photoelectrons in terms of density matrix and statistical tensor formalism. The resulting expansion over spherical harmonics includes all multipoles, though its practical application becomes rather cumbersome beyond the  $E2+M1$  corrections.

In 1969, Kaplan and Markin<sup>24</sup> suggested the use of the exact interaction operator of Eq. (1), instead of a truncated expansion, in short-wavelength photoionization. This approach corresponds to the inclusion of all multipole moments and, in its computational aspects, is simpler to use than the truncated series of Eq. (2). In Ref. 24, the angular distribution of ejected electrons from a fixed-in-space  $\text{H}_2$  molecule and the total cross section were calculated in the photon en-

ergy range up to 5 keV. The resulting angular distribution represents oscillations due to the interference of two electrons emitted from different atoms. The number of maxima and minima rises with increasing photon energy and depends upon the internuclear distance. In a subsequent study,<sup>25</sup> a full relativistic calculation of the photoionization of  $\text{H}_2$  in the  $\gamma$ -ray range with  $E_{\text{ph}} \leq 1$  MeV was performed.

To the best of our knowledge, the nonexpanded exponential operator of Eq. (1) has not been employed in atomic or molecular photoionization studies since the publication of Refs. 24 and 25. In the present study, we use Kaplan and Markin's<sup>24</sup> approach with the plane-wave approximation for the ejected electron, but reformulate it within the framework of electron propagator theory.

The electron propagator theory (EPT) provides a computationally efficient and conceptually transparent approach to the photoionization problem.<sup>26</sup> Electron binding energies including final-state orbital relaxation as well as electron correlation effects arise naturally from the solutions of the Dyson equation. To each of these binding energies is associated a one-electron wave function, known as a Dyson orbital, which is rigorously related to the initial and final states and which provides a one-electron interpretation of the ionization spectra.

EPT methods have been applied routinely to the calculation of electron binding energies.<sup>27-30</sup> On the other hand, calculations of photoionization intensities based on EPT are less common,<sup>26,31-35</sup> and only recently has this kind of calculation been introduced in a generally available quantum chemistry package.<sup>26</sup> All of these calculations employ the DA for representing the ionizing radiation. The so-called sudden approximation, in which the photoelectron is represented by a plane wave, is also made in these works. A superior description would be given by a Coulomb wave representation of the photoelectron or by use of the polarization propagator to describe bound-continuum transitions.

This paper reports the first calculations of differential cross sections of molecular photoionization within the framework of EPT including multipole effects. Employment of the complete operator of Eq. (1) corresponds to accounting for all multipole transitions. The theoretical photoionization cross sections based on Eq. (1) are valid in a broad interval of photon energies, from visible light up to x rays. Therefore, we present here an analysis of the angular distribution of the ejected electrons in the photoionization of the first-row hydrides  $\text{CH}_4$ ,  $\text{NH}_3$ ,  $\text{H}_2\text{O}$ , and  $\text{HF}$  in the photon energy range of 300–5000 eV. The sudden approximation is made here as well; we defer consideration of an improved description of the photoelectron to subsequent studies.

## II. THEORY

### A. Electron propagator theory

In EPT, one searches for the poles (i.e., the energies where singularities lie) of the propagator, which correspond to the ionization energies (IEs) and electron affinities (EAs) of the system under investigation. This process is equivalent to solving the pseudoeigenvalue problem<sup>27</sup>

$$[F + \Sigma(\varepsilon_n)]|g_n\rangle = \varepsilon_n|g_n\rangle, \quad (7)$$

where the Fock operator  $F$  is supplemented by the energy-dependent, nonlocal self-energy operator  $\Sigma(E)$  which includes relaxation and correlation effects. The eigenvalues of this equation,  $\varepsilon_n$ , are the electron binding energies (IEs and EAs), while the eigenfunctions are the respective Dyson orbitals (DOs) which, for the IE case, can be considered to be overlaps between the initial  $N$ - and the final  $(N-1)$ -electron states. The integral is over the coordinates of all electrons except one ( $x_1$ ), yielding a one-electron wave function that can be written as a linear combination of canonical Hartree-Fock (HF) molecular orbitals ( $\phi_i$ ),

$$|g_n\rangle = \sum_{i=1}^N |\phi_i\rangle \langle \Psi_n^{N-1} | a_i | \Psi_0^N \rangle = \sum_{i=1}^N b_{in} \phi_i. \quad (8)$$

The latter expression also is discussed in our previous paper.<sup>26</sup>

## B. Photoionization cross sections

In the EPT formulation above, and describing the wave function for a photoelectron with momentum  $\mathbf{k}_e$  by a plane wave normalized in a large cubic box of edge  $L$ ,

$$\varphi_{\mathbf{k}_e} = \frac{1}{\sqrt{L^3}} \eta_{\mathbf{k}_e}(\mathbf{r}), \quad (9)$$

where

$$\eta_{\mathbf{k}_e}(\mathbf{r}) = e^{i(\mathbf{k}_e \cdot \mathbf{r})}, \quad (10)$$

the differential cross section for the photoionization of an electron in the solid angle  $d\Omega_e$  can be written as<sup>26</sup>

$$\frac{d\sigma(\Theta)}{d\Omega_e} = \left( \frac{m_e}{\hbar^2} \right) \frac{L^3 k_e c}{2\pi\omega c} |\langle g_n | \hat{V} | \varphi_{\mathbf{k}_e} \rangle|^2, \quad (11)$$

where the operator for the interaction between light and matter is given by Eq. (1).

Because the plane wave is an eigenfunction of the momentum operator, one can rewrite Eq. (11) as

$$\frac{d\sigma(\Theta)}{d\Omega_e} = \left( \frac{e^2}{m_e} \right) \frac{k_e}{2\pi\omega c} |\mathbf{n} \cdot \mathbf{P}|^2, \quad (12)$$

where, in the general case,

$$\mathbf{P} = i\mathbf{k}_e \langle g_n | e^{i(\mathbf{k}_{ph} \cdot \mathbf{r})} | e^{i(\mathbf{k}_e \cdot \mathbf{r})} \rangle. \quad (13)$$

If the incident light is unpolarized, one must average over incident photon polarizations so that

$$|\mathbf{n} \cdot \mathbf{P}|^2 = \frac{1}{2} (|\mathbf{n}_1 \cdot \mathbf{P}|^2 + |\mathbf{n}_2 \cdot \mathbf{P}|^2). \quad (14)$$

The two polarization directions  $\mathbf{n}_1$  and  $\mathbf{n}_2$  are perpendicular to the photon propagation direction defined by  $\mathbf{k}_{ph}$ , such that  $\mathbf{n}_1, \mathbf{n}_2$ , and  $\mathbf{k}_{ph}/|\mathbf{k}_{ph}|$  define a new coordinate system in which we can define  $|\mathbf{P}|^2$  as

$$|\mathbf{P}|^2 = |\mathbf{n}_1 \cdot \mathbf{P}|^2 + |\mathbf{n}_2 \cdot \mathbf{P}|^2 + \frac{|\mathbf{k}_{ph} \cdot \mathbf{P}|^2}{|\mathbf{k}_{ph}|^2}, \quad (15)$$

so that

TABLE I. Optimized geometries and energies (a.u.).

Molecule	Geometry	$E(R(\text{HF}))$
CH <sub>4</sub>	$R(\text{CH})=1.085 \text{ \AA}$ $A(\text{HCH})=109.47^\circ$	-40.209 020 3093
NH <sub>3</sub>	$R(\text{NH})=1.011 \text{ \AA}$	-56.210 103 8236
H <sub>2</sub> O	$A(\text{HNH})=105.95^\circ$ $R(\text{OH})=0.959 \text{ \AA}$	-76.046 350 3043
HF	$A(\text{HOH})=103.50^\circ$ $R(\text{HF})=0.918 \text{ \AA}$	-100.046 444 791

$$\frac{d\sigma(\Theta)}{d\Omega_e} = \left( \frac{e^2}{m_e} \right) \frac{k_e}{4\pi\omega c} \left( |\mathbf{P}|^2 - \frac{|\mathbf{k}_{ph} \cdot \mathbf{P}|^2}{|\mathbf{k}_{ph}|^2} \right). \quad (16)$$

Integration of Eq. (16) over the solid angle  $d\Omega_e$  gives the photoionization cross section at a specific angle  $\Theta$  between the photon and photoelectron propagation directions.

By using the full exponential operator of Eq. (1), the  $\mathbf{P}$  vector can be written as

$$\mathbf{P} = i\mathbf{k}_e \langle g_n | e^{i[(\mathbf{k}_{ph} + \mathbf{k}_e) \cdot \mathbf{r}]} \rangle, \quad (17)$$

which is equivalent to including all multipole moments in the exponential expansion of Eq. (2).<sup>24</sup> For gaseous molecules with random orientations, one must integrate over the circle formed by rotating  $\mathbf{k}_e$  by  $360^\circ$  around  $\mathbf{k}_{ph}$  to consider all combinations of  $\mathbf{k}_e$  and  $\mathbf{k}_{ph}$  that conserve the angle  $\Theta$  between the photon and photoelectron propagation directions.

## III. COMPUTATIONAL METHODS

Calculations were done for the first-row hydrides CH<sub>4</sub>, NH<sub>3</sub>, H<sub>2</sub>O, and HF. All geometries were optimized at the MP2 level,<sup>36,37</sup> with the correlation-consistent triple- $\zeta$  (cc-pVTZ) basis set.<sup>38</sup> The electron propagator and cross-section calculations were done with the 6-311g( $d,p$ ) basis set.<sup>39</sup> In both cases, the full set of Cartesian Gaussian  $d$  and  $f$  functions was used. The nondiagonal, renormalized, second-order<sup>40</sup> (NR2) electron propagator approximation was used to calculate the ionization potentials and to obtain the DOs needed for the cross-section calculations. A modified version of the GAUSSIAN 03 program was used.<sup>41</sup>

Cross sections were calculated for photon energies of 0.3–5.0 keV for CH<sub>4</sub>, 0.4–5.0 keV for NH<sub>3</sub>, and 0.5–5.0 keV for H<sub>2</sub>O and HF, and at angles between the photon and photoelectron propagation directions of  $\Theta=90^\circ$  and  $54.74^\circ$  [the so-called dipole magic angle MA]. Relativistic effects were not included. Since the cross sections become smaller as the photon energy increases, a relative integral convergence criterion was used, with the integration being considered converged when the difference between two consecutive integrals is below 0.01%.

## IV. RESULTS AND DISCUSSION

Table I shows the optimized geometries, while Table II shows the ionization energy and pole strength results for the NR2 EPT calculations. The results are in good agreement with previous calculations and with experiments.<sup>26</sup> Larger

TABLE II. Ionization Energies in eV and pole strengths (PS) in parentheses.

Molecule	Orbital	Theory (PS)	Expt.
CH <sub>4</sub>	1a <sub>1</sub>	291.81 (0.79)	290.7 <sup>a</sup>
	2a <sub>1</sub>	22.92 (0.82)	23.0
	1t <sub>2</sub>	14.08 (0.92)	14.0
NH <sub>3</sub>	1a <sub>1</sub>	406.81 (0.80)	405.6 <sup>a</sup>
	2a <sub>1</sub>	29.63 (0.22)	
		26.99 (0.57)	27.7
	1e	16.16 (0.93)	16.5
H <sub>2</sub> O	3a <sub>1</sub>	10.39 (0.92)	10.85
	1a <sub>1</sub>	541.05 (0.81)	539.7 <sup>b</sup>
	2a <sub>1</sub>	37.37 (0.10)	
		32.81 (0.62)	32.2
		30.21 (0.12)	
	1b <sub>2</sub>	18.48 (0.94)	18.4
	3a <sub>1</sub>	14.28 (0.93)	14.7
HF	1b <sub>1</sub>	12.00 (0.92)	12.6
	1σ	695.14 (0.83)	694.0 <sup>c</sup>
	2σ	40.94 (0.40)	
		38.08 (0.49)	39.65
	3σ	19.44 (0.94)	19.89
	1π	15.41 (0.93)	16.12

<sup>a</sup>Reference 42.<sup>b</sup>Reference 43.<sup>c</sup>Reference 44 and 45.

discrepancies are expected for the core ionization energies, for the NR2 approximation gives an incomplete description of orbital relaxation in final states.

The effects of the multipole terms were estimated as a percent difference ( $\Delta\%$ ) between the multipole and dipole results,

$$\Delta\% = \frac{|(d\sigma_{\text{mult}}/d\Omega_e) - (d\sigma_{\text{dip}}/d\Omega_e)| \times 100}{(d\sigma_{\text{dip}}/d\Omega_e)}, \quad (18)$$

and this function is shown in Figs. 1–4. Each calculation is represented by a point, and the lines, derived from a cubic

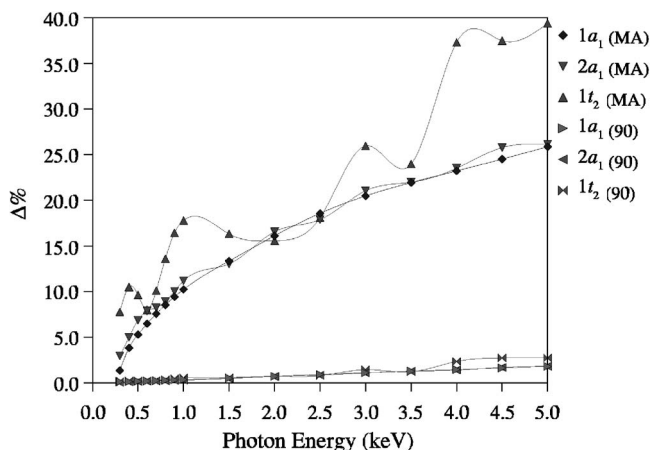


FIG. 1. Estimates of multipole effects for the CH<sub>4</sub> molecule, as defined in Eq. (18). The quantity in parenthesis indicates the angle  $\Theta$  between the photon and photoelectron propagation directions, in degrees. MA stands for the so-called magic angle (54.74°). The lines are derived from a cubic spline fit, and are intended only as guides.

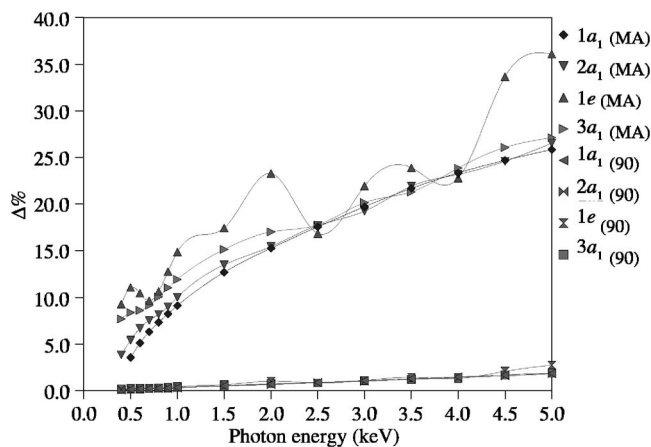


FIG. 2. Estimates of multipole effects for the NH<sub>3</sub> molecule, as defined in Eq. (18). The quantity in parenthesis indicates the angle  $\Theta$  between the photon and photoelectron propagation directions, in degrees. MA stands for the so-called magic angle (54.74°). The lines are derived from a cubic spline fit, and are intended only as guides.

spline fit, are intended only as guides. The respective DOs were depicted in Figs. 1–4 of Ref. 26.

The results in Figs. 1–4 compare the DA with the full inclusion of all multipole moments in the expansion of Eq. (2). To estimate the importance of different terms in the expansion, it is useful to analyze the results using Eq. (6). At an angle of  $\Theta=57.74^\circ$  between the photon and photoelectron propagation directions, the second term in brackets in Eq. (6) (the dipole term) vanishes, and the difference between the dipole and multipole calculations is due only to terms of higher order, that is, to all the terms higher than dipole in the expansion of Eq. (2). When the detector is positioned at an angle of  $\Theta=90.0^\circ$  from the photon propagation direction, the electric quadrupole ( $E2$ ) and magnetic dipole ( $M1$ ) terms also vanish, meaning that the difference now is due only to terms of even higher orders.

The first feature to be noted in Figs. 1–4 is the rising contribution of the multipole terms with increasing photon energy. Because the DA fails at large photon energies, this

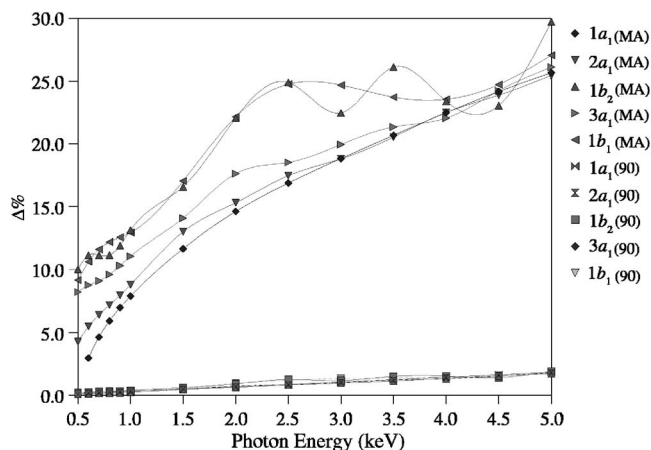


FIG. 3. Estimates of multipole effects for the H<sub>2</sub>O molecule, as defined in Eq. (18). The quantity in parenthesis indicates the angle  $\Theta$  between the photon and photoelectron propagation directions, in degrees. MA stands for the so-called magic angle (54.74°). The lines are derived from a cubic spline fit, and are intended only as guides.

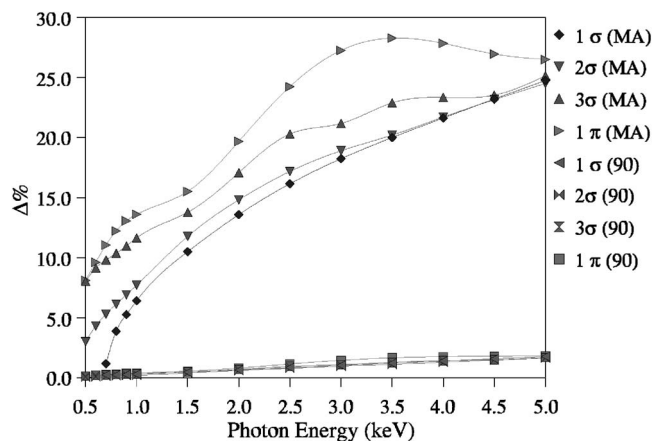


FIG. 4. Estimates of multipole effects for the HF molecule, as defined in Eq. (18). The quantity in parenthesis indicates the angle  $\Theta$  between the photon and photoelectron propagation directions, in degrees. MA stands for the so-called magic angle ( $54.74^\circ$ ). The lines are derived from a cubic spline fit, and are intended only as guides.

effect is expected. At energies about 1.5 keV, the wavelength is of the same order of magnitude as the linear dimension of a small molecule. At the highest energy considered in this study (5000 eV), the multipole contribution is most often around 25%, reaching 39% for the photoionization from the  $1t_2$  orbital in  $\text{CH}_4$  and 36% for the photoionization from the  $1t_2$  orbital in  $\text{NH}_3$ . At such photon energies, the relativistic correction can become non-negligible.<sup>7</sup>

The contributions from terms of higher orders than those presented in Eq. (6) are quite small. For valence orbitals, they are about 0.5% at 1000 eV and reach 2.7% at 5000 eV. Because these terms are of second order in the wave vector  $k = \omega/c$ , such results are not surprising. However, despite their small magnitude, high multipole contributions have been revealed in photoionization measurements.<sup>17,20</sup> For the Ne atom,<sup>17</sup> second-order nondipole effects have been demonstrated experimentally by angular distributions of ejected valence electrons. Comparison of the measured angular distributions of emitted photoelectrons from an  $\text{N}_2$  molecule fixed in space<sup>20</sup> with theoretical estimates based on first-order terms in  $k$  in Eq. (6) has shown that multipoles of higher order must be included to obtain agreement between theory and experiment.

Another important aspect to be considered is the nature of the orbital being ionized. For core orbitals, the multipole effect grows monotonically in the range studied. In all cases, the DOs are dominated by the  $1s$  orbital of the heavy atom and are very localized, making valid the argument that the wavelength of the radiation is much larger than the target size.

It has been shown that, for atoms, the more nodes the wave function has, the more oscillations should appear in the multipole corrections.<sup>9,10,46</sup> Increases in the atomic number and the principal quantum number also have been shown to increase the oscillations.<sup>46</sup> The results from Figs. 1–4 show the molecular counterpart for this effect: as contributions from outer atomic orbitals become important, oscillations in the multipole corrections appear.

In the case of  $\text{CH}_4$ , this effect is easily noticed for the  $1t_2$

DO, which is dominated by the C  $2p$  atomic orbital. The  $2a_1$  orbital is dominated by the C  $2s$  orbital and also shows oscillations, although of lower amplitude due to some contribution from C  $1s$ . The  $1t_2$  orbitals have a nodal plane that is absent in  $2a_1$  and which further amplify the multipole effects.

The same trend is seen for  $\text{NH}_3$ . The strong oscillations in the multipole effect in the  $1e$  orbital can be explained by the dominant role of the N  $2p_{x,y}$  orbitals. The outermost,  $3a_1$  orbital is composed chiefly of the N  $2p_z$  orbital, but with some contribution from N  $1s$  and  $2s$ , which quench the oscillations.

In the case of water, the orbitals most affected by the multipole corrections are  $1b_2$  and  $1b_1$ , in this order. An analysis of the components of the DOs show that the  $1b_1$  orbital is almost exclusively formed from the O  $2p_x$  orbital, while the  $1b_2$  is formed from O  $2p_y$  with important contributions from the H  $1s$  orbitals. As a consequence, the  $1b_2$  orbital is three centered and more spatially extended than the  $1b_1$  orbital. Therefore, the oscillations in the  $1b_2$  multipole effects are higher than in  $1b_1$ , even though  $1b_1$  is the outermost orbital. The  $3a_1$  orbital is formed mainly by O  $2p_z$ , with mixing from O  $1s$  and  $2s$  and from H  $1s$ . The presence of O  $ns$  contributions quenches the oscillations for this orbital. The oscillations for the  $2a_1$  orbital, being mainly formed by the O  $2s$ , are very weak, and are made noticeable only by the small contribution from O  $2p_z$ .

For the HF molecule, the multipole effects are stronger for the  $1\pi$  orbital, which is formed exclusively from F  $2p_{x,y}$  functions. Weak oscillations can be noticed for the  $3\sigma$  orbital, formed from a combination of F  $2p_z$  with H  $1s$ , with smaller mixings from F  $1s$  and  $2s$ . The latter mixings do lower the intensity of the oscillations, but are balanced by the spatial extent of the orbital given by the H  $1s$  contribution. The  $2\sigma$  DO is formed almost exclusively by F  $2s$ , and the slightly noticeable oscillations are produced by a small contribution from F  $2p_z$ .

For all molecules, the second-order corrections also show an oscillatory behavior that closely follows the first-order ones, but with much smaller amplitudes.

## V. CONCLUSIONS

Multipole corrections to the dipole approximation for the angular distribution of ejected electrons in the photoionization of first-row hydrides were determined using electron propagator theory and by considering the full multipole expansion for the incident photon representation. The relative importance of first- and second-order corrections has been estimated. While the second-order corrections are always very small, below 3% in the whole range studied, the first-order corrections are more important, being significant even at energies less than 500 eV. Accurate interpretations of angle-resolved photoelectron spectra of molecules should take first-order corrections into consideration.

These corrections oscillate with photon energy and depend on the atomic constituents and spatial distribution of the Dyson orbital. As the photon energy rises, the dipole approximation becomes less valid and the background in-

creases monotonically for all ionizations. The  $1s$  atomic orbitals are highly localized, and the multipole effect on core Dyson orbitals is due chiefly to the decrease in photon wavelength. For valence ionizations, the effects of nodes in the less localized  $2s$  and  $2p$  atomic components of the Dyson orbitals lead to oscillations in the multipole corrections as functions of photon energy. Interference between functions on different nuclei also produce nodes in Dyson orbitals and thereby contribute to the importance of multipole corrections.

## ACKNOWLEDGMENT

The National Science Foundation supported this work through Grants Nos. CHE-0135823 and CHE-0451810 to Kansas State University.

- <sup>1</sup>H. Bethe and H. H. Salpeter, *Quantum Mechanics of One- and Two-Electron Atoms* (Springer, Berlin, 1957).
- <sup>2</sup>A. S. Davydov, *Quantum Mechanics* (Pergamon, Oxford, 1965).
- <sup>3</sup>I. G. Kaplan and A. P. Markin, *Opt. Spectrosc.* **24**, 475 (1968).
- <sup>4</sup>I. G. Kaplan and A. P. Markin, *Opt. Spectrosc.* **25**, 275 (1968).
- <sup>5</sup>N. L. S. Martin, D. B. Thompson, R. P. Bauman, C. P. Caldwell, M. O. Krause, S. P. Frigo, and M. Wilson, *Phys. Rev. Lett.* **81**, 1199 (1998).
- <sup>6</sup>J. Cooper and R. N. Zare, *J. Chem. Phys.* **48**, 942 (1968).
- <sup>7</sup>H. K. Tseng, R. H. Pratt, S. Yu, and A. Ron, *Phys. Rev. A* **17**, 1061 (1978).
- <sup>8</sup>W. S. Wang, Y. S. Kim, R. H. Pratt, and A. Ron, *Phys. Rev. A* **25**, 857 (1982).
- <sup>9</sup>A. Bechler and R. H. Pratt, *Phys. Rev. A* **42**, 6400 (1990).
- <sup>10</sup>A. Bechler and R. H. Pratt, *Phys. Rev. A* **39**, 1774 (1989).
- <sup>11</sup>J. W. Cooper, *Phys. Rev. A* **47**, 1841 (1993).
- <sup>12</sup>J. W. Cooper, *Phys. Rev. A* **42**, 6942 (1990).
- <sup>13</sup>J. W. Cooper and S. T. Manson, *Phys. Rev.* **177**, 157 (1969).
- <sup>14</sup>M. O. Krause, *Phys. Rev.* **177**, 151 (1969).
- <sup>15</sup>F. G. Wuilleumier and M. O. Krause, *Phys. Rev. A* **10**, 242 (1974).
- <sup>16</sup>D. W. Lindle and O. Hemmers, *J. Electron Spectrosc. Relat. Phenom.* **100**, 297 (1999).
- <sup>17</sup>A. Devianko, O. Hemmers, S. Oblad *et al.*, *Phys. Rev. Lett.* **84**, 2116 (2000).
- <sup>18</sup>J. Feagin, *Phys. Rev. Lett.* **88**, 043001 (2002).
- <sup>19</sup>O. Hemmers, H. Wang, P. Focke, I. A. Sellin, D. W. Lindle, J. C. Arce, J. A. Sheehy, and P. W. Langhoff, *Phys. Rev. Lett.* **87**, 273003 (2001).
- <sup>20</sup>R. Guillemin, H. Hemmers, D. W. Lindle *et al.*, *Phys. Rev. Lett.* **89**, 033002 (2002).
- <sup>21</sup>P. W. Langhoff, J. C. Arce, J. A. Sheehy, O. Hemmers, H. Wang, P. Focke, I. A. Sellin, and D. W. Lindle, *J. Electron Spectrosc. Relat. Phenom.* **114–116**, 23 (2001).
- <sup>22</sup>P. W. Langhoff, J. C. Arce, and J. A. Sheehy, *J. Electron Spectrosc. Relat. Phenom.* **123**, 117 (2002).
- <sup>23</sup>A. N. Grum-Grzhimailo, *J. Phys. B* **36**, 2385 (2003).
- <sup>24</sup>I. G. Kaplan and A. P. Markin, *Sov. Phys. Dokl.* **14**, 36 (1969).
- <sup>25</sup>I. G. Kaplan and A. P. Markin, *Sov. Phys. JETP* **37**, 216 (1973).
- <sup>26</sup>G. M. Seabra, I. G. Kaplan, V. G. Zakrzewski, and J. V. Ortiz, *J. Chem. Phys.* **121**, 4143 (2004).
- <sup>27</sup>J. V. Ortiz, V. G. Zakrzewski, and O. Dolgounitcheva, in *Conceptual Perspectives in Quantum Chemistry*, edited by J.-L. Calais and E. Kryachko (Kluwer, Dordrecht, 1997), Vol. 3, p. 465.
- <sup>28</sup>J. V. Ortiz, *Adv. Chem. Phys.* **33**, 35 (1999).
- <sup>29</sup>A. M. Ferreira, G. Seabra, O. Dolgounitcheva, V. G. Zakrzewski, and J. V. Ortiz, in *Quantum Mechanical Predictions of Thermochemical Data*, edited by J. Cioslowski (Kluwer, Dordrecht, 2001), p. 131.
- <sup>30</sup>J. Linderberg and Y. Öhrn, *Propagators in Quantum Chemistry*, 2nd ed. (Wiley Interscience, Hoboken, New Jersey, 2004).
- <sup>31</sup>G. D. Purvis and Y. Öhrn, *J. Chem. Phys.* **62**, 2045 (1975).
- <sup>32</sup>B. T. Pickup, *Chem. Phys.* **19**, 193 (1977).
- <sup>33</sup>G. Born and Y. Öhrn, *Phys. Scr.* **21**, 378 (1980).
- <sup>34</sup>M. K. Mishra and Y. Öhrn, *Int. J. Quantum Chem., Quantum Chem. Symp.* **14**, 335 (1980).
- <sup>35</sup>M. Deleuze, B. T. Pickup, and J. Delhalle, *Mol. Phys.* **83**, 655 (1994).
- <sup>36</sup>C. Moller and M. S. Plesset, *Phys. Rev.* **46**, 618 (1934).
- <sup>37</sup>A. Szabo, and N. S. Ostlund, *Modern Quantum Chemistry. (Introduction to Advanced Electronic Structure Theory)* (Dover, New York, 1996).
- <sup>38</sup>T. H. Dunning, Jr., *J. Chem. Phys.* **90**, 1007 (1989).
- <sup>39</sup>R. Krishnan, J. S. Binkley, R. Seeger, and J. A. Pople, *J. Chem. Phys.* **72**, 650 (1980).
- <sup>40</sup>J. V. Ortiz, *J. Chem. Phys.* **108**, 1008 (1998).
- <sup>41</sup>GAUSSIAN 2003, M. J. Frisch, G. W. Trucks, H. B. Schlegel, *et al.* Pittsburgh, PA, 2003.
- <sup>42</sup>D. A. Allison and R. G. Cavell, *J. Chem. Phys.* **68**, 593 (1978).
- <sup>43</sup>K. Siegbahn, C. Nordling, G. Johansson, *et al.* *ESCA Applied to Free Molecules*, (North-Holland, Amsterdam, 1969).
- <sup>44</sup>M. S. Banna, B. E. Mills, D. W. Davis, and D. A. Shirley, *J. Chem. Phys.* **61**, 4780 (1974).
- <sup>45</sup>M. S. Banna and D. A. Shirley, *J. Chem. Phys.* **63**, 4759 (1975).
- <sup>46</sup>M. Jung, B. Kräassig, D. S. Gemmell, E. P. Kanter, T. LeBrun, S. H. Southworth, and L. Young, *Phys. Rev. A* **54**, 2127 (1996).